DAMPING MECHANISM OF THE GIANT DIPOLE RESONANCE IN HOT NUCLEI WITH $A = 130$*

O. Wieland[a], A. Bracco[a], F. Camera[a], G. Benzoni[a], N. Blasi[a]
F.C.L. Crespi[a], S. Leoni[a], B. Million[a], S. Barlini[b]
V.L. Kravchuk[b], F. Gramegna[b], A. Lanchais[b], A. Maj[c]
M. Kmiecik[c], G. Casini[d], M. Chiari[d], A. Nannini[d], M. Bruno[e]
E. Geraci[e]

[a]Dipartimento di Fisica, Universitá di Milano
and Istituto Nazionale di Fisica Nucleare Sezione di Milano, Italy
[b]Istituto Nazionale di Fisica Nucleare, Laboratori Nazionali di Legnaro, Italy
[c]Institute of Nuclear Physics, Polish Academy of Sciences, Poland
[d]Istituto Nazionale di Fisica Nucleare Sezione di Firenze, Italy
[e]Universita' di Bologna and INFN Sez. di Bologna, Italy

(Received December 12, 2006)

The γ decay of the Giant Dipole Resonance (GDR) in ^{132}Ce nuclei has been measured using the reactions ^{64}Ni ($E_{\rm lab} = 300, 400, 500$ MeV) + ^{68}Zn and ^{16}O ($E_{\rm lab} = 130, 250$ MeV) + ^{116}Sn. The analysis of the data shows clearly that the GDR width increases steadily with temperature at least up to 4 MeV of the temperature. The data can be well interpreted within the thermal shape fluctuation model.

PACS numbers: 24.30.Cz, 24.10.Pa, 24.60.Dr, 27.60.+j

1. Introduction

The measurement of the γ-decay of the GDR gives the possibility to observe basic nuclear structure properties at finite temperature and angular momentum, such as nuclear shapes and thermal effects [1–3]. In particular, the dependence of the GDR width on temperature and angular momentum provides information on the evolution of the nuclear shapes and of the damping mechanisms of this collective state. In general, the measured GDR width is well described within the thermal shape fluctuation model (TFM) [4, 5] for $T < 2$ MeV, while at higher temperature the situation is more complex

* Presented at the Zakopane Conference on Nuclear Physics, September 4–10, 2006, Zakopane, Poland.

and not fully understood [6–13]. The present work addresses the problem at $T > 2$ MeV by measuring high energy γ-rays from the decay of the GDR. The used set-up allowed coincidence measurements with *(i)* light charged particles to identify the possible presence of pre-equilibrium emission and for a proper definition of the compound nucleus (CN) temperature, and with *(ii)* evaporation residues to select the fusion-evaporation channel. The experiment has been performed at the Legnaro National Laboratory of the INFN. Two different reactions, the symmetric ^{64}Ni (300, 400, 500 MeV) + ^{68}Zn and the asymmetric one ^{16}O (130, 250 MeV) + ^{116}Sn were employed. These reactions produce the compound nucleus ^{132}Ce at the excitation energy of 200, 150 and 100 MeV. The used experimental setup consists of the GARFIELD array [14] for light charged particle detection (LCP) combined with the large volume BaF_2 detectors of the HECTOR set up [16] for high energy γ-ray detection and two Position Sensitive Parallel Plate Avalanche Counter telescopes (PSPPAC) for heavy residues selection. The reactions use the same tagging conditions, deduced from the PPACs identification of the recoiling residues, both for the light charged particles and for the γ-rays.

2. Results

In Fig. 1 (left) the time of flight (TOF) spectra of the BaF_2 detectors is shown. The good time resolution allows to distinguish the prompt γ events from neutrons emitted in the collisions.

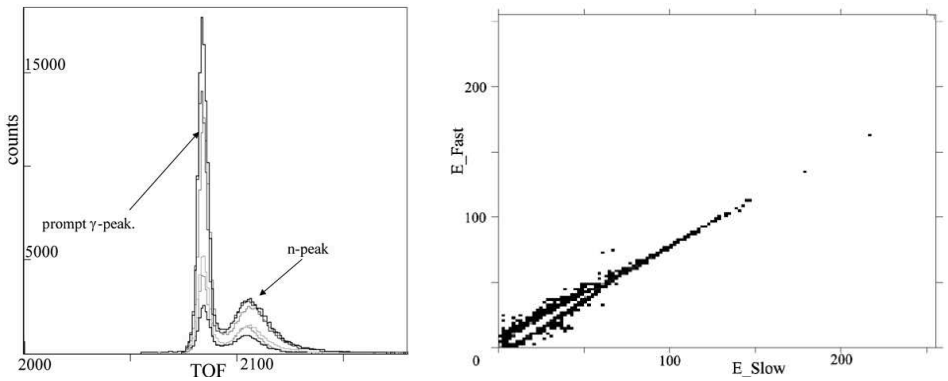


Fig. 1. Left: Time of flight spectra measured with the BaF_2 detectors positioned at 30 cm distance from the target (0.1 ns per channel). Right: Two dimensional spectra of the fast component *versus* slow light output of the BaF_2 detectors.

In Fig. 1 (right) the fast light output component of one BaF_2 detector versus the slow signal is shown in a 2 dimensional plot. Practically no LCP background events besides the main central line, which is originated from

γ-ray interactions, is present. In Fig. 2 the α-particle spectra measured at different angles in both the symmetric and asymmetric reactions are displayed. It is important to stress that the value of the excitation energy deduced from kinematics is the same for the two reactions, namely for the ^{16}O + ^{116}Sn at $E_{\rm beam} = 250$ MeV (Fig. 2 (left)) and for the ^{64}Ni + ^{68}Zn at $E_{\rm beam} = 500$ MeV (Fig. 2 (right)).

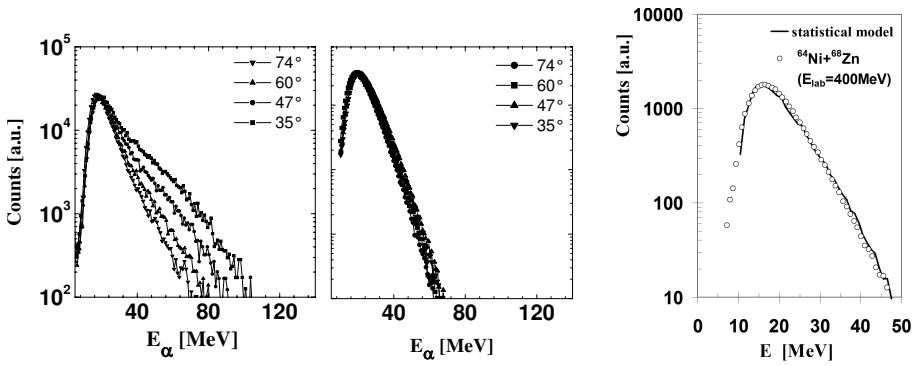


Fig. 2. Measured α-particle spectra in the CM frame system at different detection angles for the ^{16}O-induced reaction ($E_{\rm lab} = 250$ MeV) (left) and for the ^{64}Ni-induced reaction ($E_{\rm lab} = 500$ MeV) (center) [17]. Measured and calculated statistical model spectra for α-particles emitted from ^{132}Ce for the ^{64}Ni-induced reaction ($E_{\rm lab} = 400$ MeV) (right).

The α-particle spectra corresponding to the ^{16}O induced reaction shows a very different spectral shape at varying angles and is strongly forward focused (Fig. 2). The spectral shape corresponding to the ^{64}Ni induced reaction, instead, is not changing with detection angles as all the spectra overlap, in addition in the ^{64}Ni case there is no sizeable pre-equilibrium emission and the spectra could be well reproduced by statistical model calculations with the PACE4 code, using default parameters, varying only the inverse nuclear temperature dependent level density parameter K with a starting value of 13 MeV [15], as can be seen in Fig. 2 (right). Extensive and detailed analyses of the LCP spectra for both symmetric and asymmetric reactions will be the subject of future papers [15, 18]. The high energy γ-ray spectra measured in coincidence with the recoiling residual nuclei from the symmetric reaction induced by the Ni beam are shown in Fig. 3 (symbols) together with the best fitting statistical model calculations (full line) [17, 19, 20]. The calculations were folded with the detector response function calculated using the GEANT [21] libraries of the BaF_2 array and were then normalized at around 8 MeV. A value of $\approx 100\%$ of the TRK sum-rule together with a single Lorentzian strength function was used. The resonance width and centroid were treated as free parameters of the fit using a χ^2 minimization

procedure between 12–22 MeV as described in Ref. [8]. For the level density description the Reisdorf formalism [23, 24] was used for the lower excitation energy part, this means the level density parameter a (MeV^{-1}) decreases between $A/9$ and $A/10$ for $E^* < 100$ MeV. For $100 < E^* < 170$ MeV a is going from $A/10$ to $A/11$ for $E^* > 170$ MeV a arrives to $A/12.5$. Since the experimental bombarding energies imply a saturation of the angular momentum of the CN an average value of $\langle J \rangle = 45\hbar$ and maximum of $L_{\max} = 70\hbar$ was used for all the present calculations.

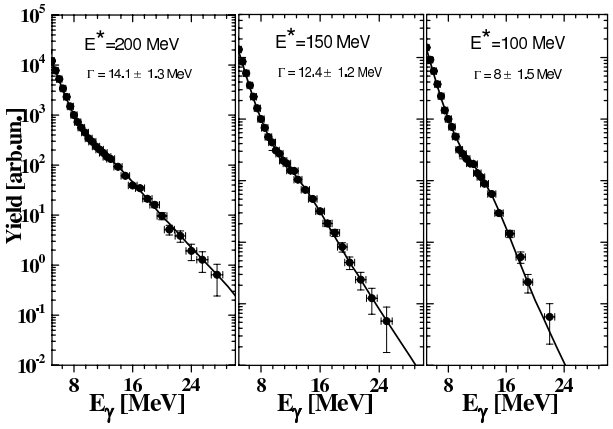


Fig. 3. The measured (points) and calculated statistical model (full line) high energy γ-ray spectra for ^{132}Ce at excitation energy of 200, 150 and 100 MeV [17].

The best fitting values of the GDR width deduced from the analysis of the GDR region are listed in Table I together with the reaction parameters. The GDR centroid have been measured at $E_{\rm GDR} \approx 14$ MeV, as already found in [22], while a clear increase of the GDR width with excitation energies (see Fig. 4) is evident. The absence of pre-equilibrium in the ^{64}Ni induced reaction fixes the excitation energy E^* of the fused CN to their kinematical values (see Table I). The nuclear temperature of the CN associated with the GDR decay have been calculated with the expression $T = 1/[d(ln(\rho))/dE]$ [12, 25, 26], where ρ is the level density. The resulting values for the present data are not substantially different from the one, calculated using the relation $T = [(E^* - E_{\rm rot} - E_{\rm GDR})/a)]^{1/2}$, where $E_{\rm rot}$ is the rotational energy. The measured and extracted GDR widths does not reflect the properties of the CN but some kind of average over all the decay paths. It is important to extract the weighted 'average' temperature of the measured GDR at which the measured high energy γ-rays were emitted, for a meaningful comparison with the GDR model predictions. A straightforward approach, followed for example in Ref. [12], defines a generic overall $\langle T \rangle$ by averaging the temperatures of all the nuclei involved in the decay weighted by their γ-ray yield

at high energy, namely between 12–20 MeV. In this work we have followed a different procedure. In fact, what is needed is the temperature associated to the GDR width extracted in the fitting procedure and not the temperature of the generic high-energy γ-ray emission. These two temperatures might be different, especially at high excitation energies. We have indeed observed that, in the fitting procedure, the value of the width of the GDR for nuclei at the end of the decay cascade does not significantly influence the results of the total fit. Namely, a change in the GDR width in all nuclei which in the decay cascade are below a threshold temperature $T_{\rm s}$ does not significatively affect the total calculated spectra. From the statistical point of view the difference of the χ^2 values remains within the intrinsic statistical uncertainties making the two spectra undistinguishable. Consequently, we have calculated an 'effective' temperature T^* which is defined as the temperature at which there is 50% of the high energy γ-ray yield (12–20 MeV) which is emitted between $T_{\rm s}$ and the temperature of the initial compound $T_{\rm CN}$. The neglected yield in the average corresponds to the decay at the end of the CN cascade which is not sensitive to the GDR width because of its spectra shape. This temperature is associated to the GDR width extracted in the fitting procedure. For high excitation energies this effective temperature corresponds to about 80% of the initial $T_{\rm CN}$ temperature [27]. Table I lists, from columns 6 to 8, these different temperatures. The effective and average temperatures are almost identical at low excitation energies, namely, when high energy γ-ray emission is concentrated in the very first steps.

TABLE I

Columns with beam energy, excitation energies and the average spin for the ^{64}Ni induced reaction, GDR parameters (in MeV), CN $T_{\rm CN}$, effective T^* and the average temperature $\langle T\rangle$.

^{64}Ni $E_{\rm beam}$	E^*	$\langle J\rangle$	$\Gamma_{\rm GDR}$	$E_{\rm GDR}$	$T_{\rm CN}$	T^*	$\langle T\rangle$
500 MeV	200 MeV	45 $\hbar$	14.1 $\pm$ 1.5	14.0	4.1	3.7	2.9
400 MeV	150 MeV	45 $\hbar$	12.4 $\pm$ 1.2	14.0	3.2	2.8	2.2
300 MeV	100 MeV	45 $\hbar$	8 $\pm$ 1.3	14.0	2.2	1.9	1.8

In Fig. 4 the measured values of the GDR width are compared with theoretical predictions based on the TFM. Within the TFM the GDR strength function is calculated by averaging the line shape corresponding to the different possible deformations and weighted with a Boltzmann factor $P(\beta,\gamma) \propto exp(-F(\beta,\gamma)/T)$ where F is the free energy and T the nuclear temperature [1, 2, 4, 5]. At each deformation point the intrinsic width Γ_0 of the resonance was chosen equal to the zero temperature value, namely 4.5 MeV. One can note that the increase does not reproduce the experimental data

(Fig. 4, thin line). The predicted increase follows rather well the deformation increase of the CN induced by temperature, (Fig. 4, dashed line, scale on the right vertical axis). An explanation for the discrepancy between the data and the TFM at $T > 2.5$ MeV could be related to the fact that the effect of the lifetime of the CN plays a role at these temperatures [28–30]. The calculations with the TFM including also the CN lifetime [28] is shown in Fig. 4 with the thick line.

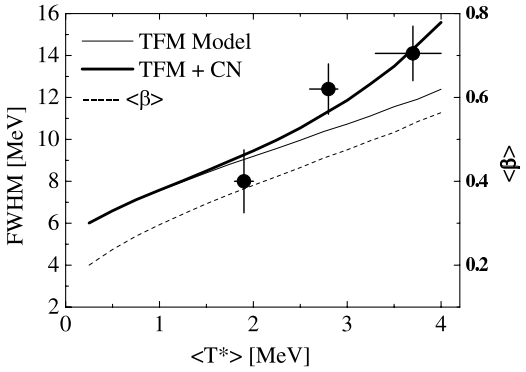


Fig. 4. Comparison between measured (points) and calculated GDR width [17]. The thick continuous line shows the predictions of the TFM with the inclusion of the CN lifetime. The continuous line indicates the results of shape fluctuation alone. The dashed line shows the average deformation $\langle\beta\rangle$ calculated by the TFM [4, 5].

A good agreement between the experimental data and the predictions is found. From the present comparison one can also note that, in agreement with the expectation of the theory [1], for $T > 2$ MeV there is no room for a significant increase of the intrinsic width Γ_0 with temperature [31], unless one unrealistically neglects the CN lifetime contribution to the total width.

3. Conclusions

The results of measurements of high energy γ-rays from the GDR built on hot compound nucleus with $A = 130$ were presented. The analysis of both, light charged particles and of the γ-rays measured in coincidence with heavy recoiling nuclei has shown that at energies of up to $E^* = 200$ MeV the symmetric reactions do not have sizable pre-equilibrium emission and consequently there is basically no cooling down of the nucleus before thermalization. The GDR width does not saturate at $T > 2.5$ MeV but increases steadily with temperature at least up to 4 MeV. Deformation effects and intrinsic lifetime of the CN are the two combined mechanisms which explain the measured increase of the width with temperature.

This work was partially supported by the Italian National Institute of Nuclear Physiscs (INFN) and by the Polish State Commitee for Scientific Research (KBN Grant No. 1 P03B 030 30).

REFERENCES

[1] P.F. Bortignon, A. Bracco, R.A. Broglia, *Giant Resonances: Nuclear Structure at Finite Temperature*, Harwood Academic Publishers, Amsterdam, 1998.
[2] F. Camera *et al.*, *Nucl. Phys.* **A572**, 401 (1994).
[3] M. Matiuzzi *et al.*, *Phys. Lett.* **B364**, 13 (1995).
[4] D. Kusnezov, E. Ormand, *Phys. Rev. Lett.* **90**, 042501-1 (2003).
[5] Y. Alhassid, *Nucl. Phys.* **A649**, 107c (1999) and references therein.
[6] J.H. Le Faou *et al.*, *Phys. Rev. Lett.* **72**, 3321 (1994).
[7] D.R. Chakrabarty *et al.*, *Phys. Rev.* **C36**, 1886 (1987).
[8] A. Bracco *et al.*, *Phys. Rev. Lett.* **62**, 2080 (1989).
[9] R.J. Voijtech *et al.*, *Phys. Rev.* **C40**, R2441 (1989).
[10] G. Enders *et al.*, *Phys. Rev. Lett.* **69**, 249 (1992).
[11] H.J. Hoffman *et al.*, *Nucl. Phys.* **A571**, 301 (1994).
[12] M.P. Kelly *et al.*, *Phys. Rev. Lett.* **82**, 3404 (1999).
[13] M.P. Kelly *et al.*, *Phys. Rev.* **C56**, 3201 (1997).
[14] F. Gramegna *et al.*, *Nucl. Instrum. Methods* **A389**, 474 (1997).
[15] A. Maj *et al.*, *Nucl. Phys.* **A571**, 185 (1994).
[16] S. Barlini *et al.*, to be published in 2007.
[17] O. Wieland *et al.*, *Phys. Rev. Lett.* **97**, 012501 (2006).
[18] V.L. Kravchuk *et al.*, IWM 2005 Conference Proceedings.
[19] F. Pülhofer, *Nucl. Phys.* **A280**, 267 (1977).
[20] I. Dioszegi, *Phys. Rev.* **C64**, 019801 (2001) and references therein.
[21] R. Brun *et al.*, CERN Report No. CERN-DD/EE/84-1.
[22] D. Pierroutsakou *et al.*, *Phys. Rev.* **C71**, 054605 (2005).
[23] W. Reisdorf, *Z. Phys.* **A300**, 227 (1981).
[24] I. Dioszegi *et al.*, *Phys. Rev.* **C63**, 047601 (2001).
[25] M. Kmiecik *et al.*, *Nucl. Phys.* **A674**, 29 (2000).
[26] M. Thoenessen, Riken Review No 23, July 1999.
[27] A. Bracco, F. Camera, COMEX-2 Conference Proceeding, *Nucl. Phys.* **A** (2006) and to be published in 2007.
[28] W.E. Ormand *et al.*, *Nucl. Phys.* **A614**, 217 (1997).
[29] Ph. Chomaz, *Phys. Lett.* **B347**, 1 (1995).
[30] Ph. Chomaz, *Nucl. Phys.* **A569**, 569 (1994).
[31] A. Bracco *et al.*, *Phys Rev. Lett.* **74**, 3748 (1995).